

Zeolitic imidazolate framework-8 (ZIF-8) for drug delivery: a critical review

Simin Feng¹, Xiaoli Zhang², Dunyun Shi³, Zheng Wang (✉)¹

¹ School of Pharmaceutical Science and Technology, Tianjin University, Tianjin 300072, China

² Central Lab, Shenzhen Second People's Hospital/The First Affiliated Hospital of Shenzhen University Health Science Center, Shenzhen 518035, China

³ Institute of Hematology, Shenzhen Second People's Hospital/The First Affiliated Hospital of Shenzhen University Health Science Center, Shenzhen 518035, China

© Higher Education Press 2021

Abstract Zeolitic imidazolate framework-8 (ZIF-8), composed of Zn ions and imidazolate ligands, is a class of metal-organic frameworks, which possesses a similar structure as conventional aluminosilicate zeolites. This material exhibits inherent porous property, high loading capacity, and pH-sensitive degradation, as well as exceptional thermal and chemical stability. Extensive research effort has been devoted to relevant research aspects ranging from synthesis methods, property characterization to potential applications of ZIF-8. This review focuses on the recent development of ZIF-8 synthesis methods and its promising applications in drug delivery. The potential risks of using ZIF-8 for drug delivery are also summarized.

Keywords zeolitic imidazolate framework-8 (ZIF-8), synthesis methods, applications, drug delivery

1 Introduction

Metal-organic frameworks (MOFs), which are composed of metals coordinated to organic ligands to form finite secondary building units (SBUs), have incessantly attracted attention in the fields of material science, pharmaceutical science, and nanotechnology [1–3]. In particular, MOFs possess modular structures and merely require mild synthesis conditions to facilitate their structural designs. By utilization of SBUs with distinct geometrical shapes, numerous functionalities can be

integrated into MOFs [4]. In addition, the topologies of MOFs can also be changed by adjusting SBUs arrangement. Zeolitic imidazolate frameworks (ZIFs) are a unique type of MOFs, which have been extensively studied in recent years. ZIFs consist of self-assembled M-IM-M structures, in which M stands for tetrahedrally-coordinated metal ions such as Co, Cu, Zn cations and IM represents the imidazolate ligand [5]. The angle of M-IM-M structure is 145° to enable a zeolite-like topology [6,7]. As they possess similar structures to conventional aluminosilicate zeolites, ZIFs exhibit properties of both MOFs and zeolites, such as exceptional thermal and chemical stability, ultrahigh surface area, high crystallinity, unimodal micropores and abundant functionalities [8]. Based on these advantages, ZIFs have been used in numerous fields, including separations [9–11], catalysis [12,13], gas storage [14–16], chemical sensors [17,18], and drug delivery. The tailored design of ZIFs responses to various stimuli, e.g., pH [19], singlet oxygen [20,21], and redox potential gradient [22]. All these characteristics make ZIFs suitable for drug delivery.

ZIF-8, composed of Zn ions and 2-methylimidazole (MIM), is one typical type of ZIFs [23], which exhibits a sodalite-type structure illustrated in Fig. 1. A micropore with a diameter of 11.6 Å is located in the center of this material, which is accessible through small apertures with a diameter of 3.4 Å. Several synthesis approaches of ZIF-8 have been proposed, including solvothermal synthesis, hydrothermal synthesis, ultrasound/sonochemical synthesis, mechanochemical synthesis, and accelerated aging methods. Because of the tunable compositions, controllable structures and high level of porosity, ZIF-8 has been applied in various applications such as catalysts, adsorbents, and drug delivery [24]. This review focuses on the synthesis methods and drug delivery application of ZIF-8.

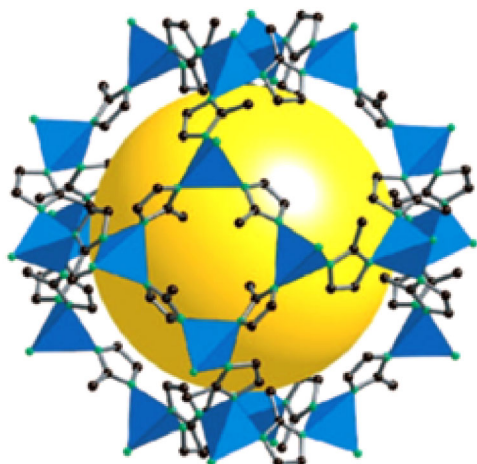


Fig. 1 The crystal structure of ZIF-8. Black and green dots represent the carbon and nitrogen atoms, respectively. Blue polyhedrons stand for the Zn ions. All hydrogen atoms are excluded here. The yellow sphere stands for the largest van der Waals sphere enclosed in the central pore of ZIF-8. Reprinted with permission from ref. [23]. Copyright 2006, the National Academy of Sciences of the USA.

2 Synthesis of ZIF-8 materials

2.1 Solvothermal synthesis

Organic solvents are employed as the reaction medium in this approach to prepare ZIF-8 materials. Park et al. [23] firstly synthesized ZIF-8 crystals using organic solvents such as *N,N*-dimethylformamide (DMF), *N*-methylpyrrolidine, and *N,N*-diethylformamide. In Fig. 2, the zinc nitrate tetrahydrate $\text{Zn}(\text{NO}_3)_2 \cdot 4\text{H}_2\text{O}$ and MIM were dissolved in DMF, and then heated up to 140°C and maintained at this temperature for 24 h [23]. However, it is challenging to remove DMF trapped inside the ZIF-8 pores by solvent exchange as the molecule size of DMF is larger than that of sodalite cage [25]. Methanol is reported to be a suitable alternative to DMF since it can be easily removed from the pores of ZIF-8 due to its smaller kinetic diameter in contrast to DMF [25]. The methanol solution containing MIM or 2-ethylimidazole was mixed with the aqueous ammonia solution containing $\text{Zn}(\text{OH})_2$ to produce ZIF crystals [26]. Based on this pioneer work, ZIF-8 crystals were prepared by mixing the same ingredients as reported at room temperature for 5 h [27,28]. It was also reported that nanoscale ZIF-8 materials can be synthesized using a molar ratio between Zn ions and MIM of 1:8 [29]. Further research found that the methanol-based synthesis of ZIF-8 could be improved by additive doping. Cravillon et al. [30] employed sodium formate/MIM and *n*-butylamine as modulating ligands to control the dimensions of ZIF-8 nanocrystals ranging from 10 to 65 nm. The modulating ligands also increased the crystallization speed of ZIF-8 at room temperature [31]. The poly-(diallyldimethylammo-

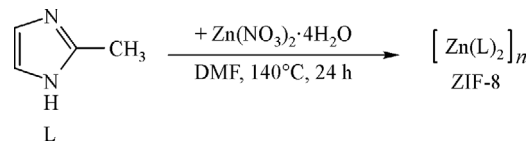


Fig. 2 Solvothermal synthesis process of ZIF-8.

nium chloride) with high molecular weight was used as a stabilizer in methanol to prepare hexagonally-shaped ZIF-8 nanocrystals [32]. Moreover, other organic solvents such as isopropyl alcohol [33] and ethanol [34] were also used for ZIF-8 preparation.

Shen et al. [35] constructed highly oriented and ordered macropores within ZIF-8 single crystals, which opens up the area of three-dimensional-ordered macro-microporous materials in single-crystalline form. The precursor@PS monoliths were prepared through filling the ZIF-8 precursors (MIM and $\text{Zn}(\text{NO}_3)_2$) into highly ordered three-dimensional PS monoliths made of monodisperse polystyrene spheres (PSs). Then precursor@PS monoliths were soaked in $\text{CH}_3\text{OH}/\text{NH}_3 \cdot \text{H}_2\text{O}$ mixed solutions to synthesize the single-crystal ordered macropore ZIF-8, namely SOM-ZIF-8. The critical and necessary process to achieve uniform SOM-ZIF-8 materials is the use of methanol/ammonia water mixtures as solvents. Methanol is largely employed in the preparation of uniform ZIF-8 materials [36,37] but it generally does not provide high synthetic yield. Pure ammonia can effectively increase the yield of ZIF-8. However, it causes too high crystallization rates and leads to formation of uniform ZIF-8 crystals [38]. In the absence of ammonia, all ZIF-8 crystals nucleate and grow outside the PS template, producing tiny solid ZIF-8 nanocrystals. Shen et al. [35] successfully realized the controlled crystallization of SOM-ZIF-8 (3, 0.5) within template-confined spaces by combining the advantages of both types of solvents.

2.2 Hydrothermal synthesis

Organic solvents used in solvothermal synthesis methods are flammable, expensive, toxic and environmentally harmful. In order to overcome these shortcomings, manufacture of ZIF-8 in a facile and green manner is needed. In recent years, the use of aqueous solutions has been explored in the synthesis of ZIF-8 at room temperature. However, dense structures without porous framework were obtained in aqueous solution, which remains as an obstacle for the synthesis of ZIF-8. Pan et al. [39] firstly solved this problem and prepared ZIF-8 at room temperature via a simple process in an aqueous system. They mixed the MIM solution with the zinc nitrate solution and stirred the mixture for about 5 min, followed by product collection through centrifugation. However, the amount of MIM is about 70 times that of Zn ions used in this method. It causes an excess waste of MIM because the

stoichiometric molar ratio between MIM and Zn ions in ZIF-8 is theoretically suggested to be 2.

The influence of the MIM/Zn molar ratios ranging from 100 to 20 on the ZIF-8 preparation was exploited [40]. A recommended value was determined to be 20 [25]. The synthesis conditions under different stoichiometric molar ratios between Zn ions and MIM were investigated. It was also found that the pH value of the synthesis solution affected the crystallization of ZIF-8. Water-based synthesis methods of ZIF-8 could be modified by using deprotonation agents such as triethanolamine (TEA), hydroxide, and ammonium to reduce the use of MIM. Gross et al. [41] synthesized ZIF-8 in an aqueous system at room temperature with the addition of TEA using a molar ratio between MIM and Zn ions of 4:1. No side-products were generated in the method. Later, both triblock copolymers poly(ethylene oxide)-poly(propylene oxide)-poly(ethylene oxide) [42] and poly-vinylpyrrolidone were used as additives for ZIF-8 formation as shown in Fig. 3. Such surfactants can aid the synthesis of ZIF-8 because of the electrostatic interaction between ZIF-8 and metal ions. The Wang group further synthesized the ZIF-8 in concentrated ammonium hydroxide aqueous solutions with a MIM/metal molar ratio of 2:1 [43]. Controlling the concentration of aqueous ammonia can tune the structures, particle sizes

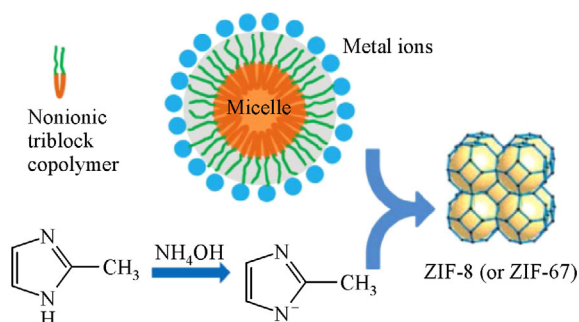


Fig. 3 Manufacture of zeolitic imidazolate frameworks (ZIF-8 and ZIF-67) in the presence of ammonium hydroxide and nonionic triblock copolymer. Reprinted with permission from ref. [42]. Copyright 2013, The Royal Society of Chemistry.

and textural properties of ZIF-8. These cost-effective synthesis methods facilitate the production of ZIF-8 materials at a large scale.

2.3 Ultrasound/Sonochemical synthesis

ZIF-8 can also be synthesized by ultrasound or sonochemical methods. Seoane et al. [44] synthesized the ZIF-8, ZIF-7, ZIF-11 and ZIF-20 crystals under ultrasound (US) and solvothermal (ST) conditions as shown in Table 1. ZIF-8 was produced at 45°C under ultrasound treatment with a frequency of 47 kHz and a power of 110 W. Compared with the traditional solvothermal methods, the duration time of ultrasound or sonochemical synthesis is shorter. It is also found that ZIF-8 crystals possess smaller particle size and narrower particle size distribution in contrast to those made by conventional solvothermal approaches [44].

By using NaOH and TEA as pH modulation agents, Cho et al. [45] prepared ZIF-8 using a sonochemical method. Under remarkably high substrate concentrations (Zn^{2+} : DMF = 1:9.3), ZIF-8 was synthesized at a large scale within 2 h. By the reasonable utilization of high substrate concentration, pH adjustment and sonochemistry, it is possible to achieve the synthesis of ZIF-8 at large scale and with high-efficiency. Furthermore, the synthesis time can be reduced from several days for traditional synthesis methods to only 1–2 h for the ultrasound or sonochemical methods [45]. The sonochemical method involves acoustic cavitation, which produces high local temperature, pressure and extraordinarily fast heat transfer. During these processes, bubbles form and collapse in solutions [46]. In contrast to the traditional oven heating for ZIF-8 synthesis, sonochemical methods accelerate the particle nucleation homogeneously in solutions [47].

2.4 Mechanochemical synthesis

Since it is a green and efficient strategy, mechanochemistry has shown significant potential for the preparation of ZIF-8 [48]. By avoiding the use of solvents and salts in the synthesis process, mechanochemical synthesis method can

Table 1 Synthesis conditions of ZIF-8, ZIF-7, ZIF-11 and ZIF-20 materials ^{a)}

ZIF	Synthesis method	Synthesis temperature/°C	Synthesis time/h
ZIF-8	US	45	4, 6, 9
	ST	140	24
ZIF-7	US	60	3
ZIF-11	US	60	6, 9, 12
	ST	100	96
ZIF-20	US	45	3, 6, 9, 12
	ST	65	72

a) Reproduced with permission from ref. [44]. Copyright 2012, The Royal Society of Chemistry.

reduce environmental contamination and reduce the incorporation of impurities into the crystal lattice. A dense Zn(IM)_2 was prepared by manually grinding of ZnO with a large amount of IM [49] or by employing a mechanochemical method using ZnCl_2 [50]. In order to overcome the oxidation due to dry grinding, the liquid-assisted or ion-assisted grinding processes were proposed for synthesis of ZIF-8 [51]. The liquid phase can enhance sliding mobility of these particles [52]. Furthermore, salt additives can facilitate the formation of ZIF-8 [53]. More importantly, the grinding liquid and salt additives may control the topology of the synthesized ZIF-8.

The mechanochemical dry conversion from ZnO to ZIF-8 was also reported without the usage of solvents and additives [54]. The mechanism of the mechanochemical synthesis of ZIF-8 is shown in Fig. 4. Nanoscale ZnO particles with an average size of 24 nm and MIM are mixed and grinded under a rotation speed of $100 \text{ r} \cdot \text{min}^{-1}$. During the grinding, the particles in the mixtures are firstly grinding into small pieces. Then, MIM and ZnO react to form ZIF-8 materials. Finally, the obtained ZIF-8 nanoparticles aggregate together. It is reported that the particle size of ZnO affects the structures of the obtained ZIF-8. All ZnO particles with a small size are transformed to ZIF-8 nanoparticles, as in case I shown in Fig. 4. However, the obtained ZIF-8 nanoparticles can include untransformed ZnO if the ZnO particles are not grinded into small size, as in case II shown in Fig. 4. Because mechanochemical dry conversion is dominated by the surface reaction, it is suggested to use nano-sized ZnO particles to produce ZIF-8 in mechanochemical synthesis methods. Cao et al. [55] claimed the fast amorphization of the prototypical ZIF-8 by ball-milling. The resultant amorphous ZIF-8 had a continuous random network topology which had a lower porosity and a higher density than its crystalline counterpart. However, its thermal stability was obviously reduced.

2.5 Accelerated aging method

As a moderate and environmentally friendly method, the accelerated aging approach has also been proposed to prepare ZIF-8 by taking advantage of the inherent mobility of molecules, which is inspired by the geological biomineralisation and mineral neogenesis [56–58]. In 2012, Cliffe et al. [59] firstly employed this method to prepare close-packed ZIFs by using benzimidazole, imidazole, MIM and 2-ethylimidazole as shown in Fig. 5. It was found that the accelerated aging method is different from the above mentioned four types of synthesis methods, as it includes at least three procedures: Salt-imidazole mixtures are firstly deliquated and then the salt additives are reacted with ZnO. Finally, the acidic imidazolium salts are formed which can also react with ZnO. The open structure intermediates could form close-packed ZIF-8 materials. It was also confirmed that the porous ZIF-8 materials could be obtained through the pulverization of the organic solvent containing diamondoid- Zn(MIM)_2 at room temperature. The reactions yield is 0.5 gram within 3–9 days. The accelerated aging method can be easily used for large scale manufacturing of ZIF-8, for which the energy and materials cost are the primary concerns [59]. Further, the one-step synthesis of ZIF-8 has been developed [60]. By adjusting diverse salt additives, for example, $(\text{Hcaf})(\text{HSO}_4)$, KHSO_4 , and $(\text{H}_2\text{Im})_2\text{SO}_4 \cdot 2\text{H}_2\text{O}$, accelerated aging could be optimized for the preparation of micro-porous materials. This work shows that both the deliquescence and the salt additives influence the accelerated aging process. The salt additives lead to the high product yield of ZIF-8 in contrast to the low production without the salt additives. Another difference is that reactions with salt additives remain to be solid; however, at the absence of these additives, the reactions remained partially deliquesced or liquefied [60].

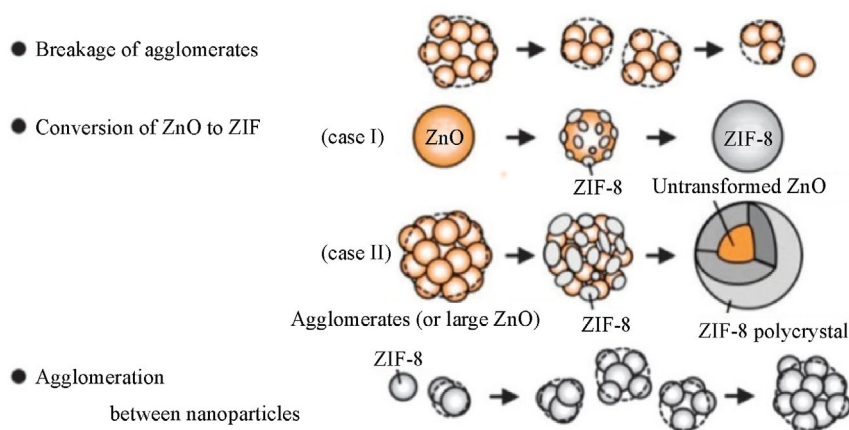


Fig. 4 Mechanochemical synthesis of ZIF-8 materials. Reprinted with permission from ref. [54]. Copyright 2013, The Royal Society of Chemistry.

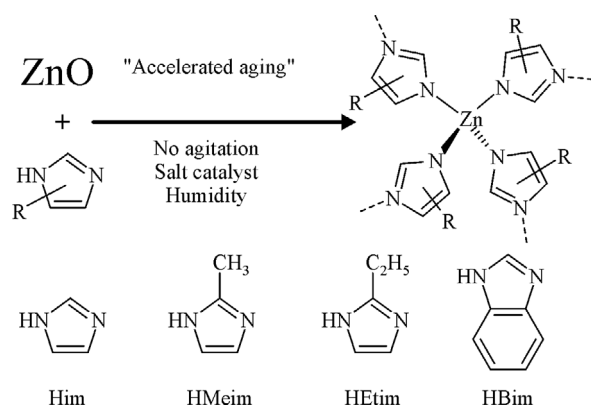


Fig. 5 The accelerated aging with selected model ligands. Reprinted with permission from ref. [59]. Copyright 2012, the Royal Society of Chemistry.

3 Applications in drug delivery

MOFs have much potential in many applications, such as catalysis [61–65], gas separation and storage [66–70], sensing [71–73], and drug delivery. All these are attributed to the attractive properties of MOFs, like structural diversity, large surface area, and tunable pore sizes and functionalities [74–77]. For the material ZIF-8, its typical properties include good dispersity, high loading capacity, excellent thermal and chemical stabilities, and pH-sensitive degradation. Sun et al. [78] reported the intriguing structure of ZIF-8 with high surface area (BET: $1630 \text{ m}^2 \cdot \text{g}^{-1}$) and large pores (11.6 \AA). ZIF-8 made of MIM and Zn ions is pH-sensitive [79,80]. Both Zn ions and MIM are physiological ingredients. Remarkably, the imidazole group is similar to the amino acid histidine and zinc is the second most common transition metal in biology [81]. The pH-triggered activation of ZIF-8 is attributed to the protonation of imidazole, resulting in the disassembly of ZIF-8. In fact, at tumor sites there is often an acidic microenvironment where pH is about 5.0–6.8. High thermal and chemical stabilities of ZIF-8 are also reported [23]. All these properties make ZIF-8 as an important vehicle in drug delivery applications. In this section, several applications of ZIF-8 as nanocarrier in drug delivery systems are summarized and discussed, as shown in Fig. 6.

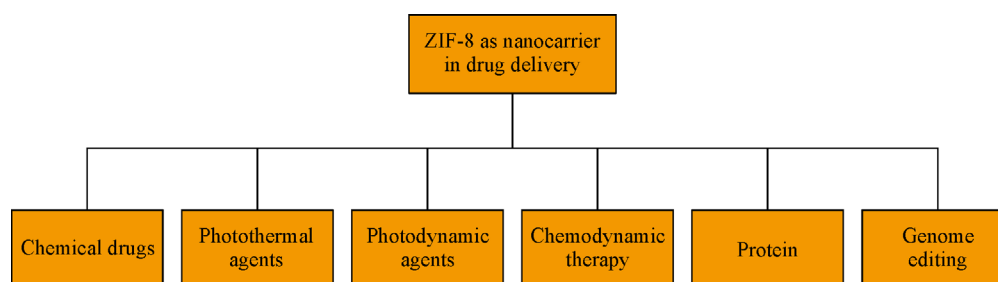


Fig. 6 Applications of ZIF-8 as nanocarrier in drug delivery.

3.1 ZIF-8 as nanocarrier for chemical drugs

According to their solubility, chemical drugs are usually divided into three categories: hydrophobic drugs, hydrophilic drugs, and amphiphilic drugs. The Zheng group proposed a simple one-pot method for the preparation of ZIF-8 to encapsulate hydrophobic drugs [82]. Based on the pH-sensitive property of ZIF-8, the doxorubicin (DOX) molecules are loaded in pores of ZIF-8. DOX@ZIF-8 circulates in the bloodstream where the pH is 7.4 in physiological states. However, DOX is gradually released upon the accumulation of DOX@ZIF-8 in tumor sites. The distinct release property of DOX@ZIF-8 makes it meaningful as an attractive pH-responsive drug delivery system for tumor treatment. Another advantage of ZIF-8 is the high loading. The anticancer drug DOX has been loaded in the ZIF-8 with a loading capacity up to 20 wt-%, as shown in Fig. 7 [82]. However, the toxicity cannot be ignored when ZIF-8 is applied in drug delivery. In Zheng's group work, after treatment with ZIF-8 at a concentration of $0.8 \mu\text{g} \cdot \text{mL}^{-1}$, the mitochondrial function dropped from the baseline level to 60% in MCF-7 cells, to 68% in MDA-MB-468 cells, and to 76% in MDA-MB-231 cells. When DOX@ZIF-8 is applied *in vivo*, the potential toxicity of ZIF-8 may be a problem that should be addressed.

DOX was also encapsulated in ZIF-8 with surface modification by poly(ethylene glycol) (PEG) and size control [83]. Similarly, a one-pot method with deionized water was used in the process, as shown in Fig. 8. In this work, the monovalent PEG-NH₂ was used as capping agent to control the size of the ZIF-8 nanoparticles through surface coordination [84]. Furthermore, the PEG molecules located on the ZIF-8 surface decrease the toxicity of ZIF-8 nanoparticles.

A simple one-step strategy has been proposed for the encapsulation of a natural hydrophobic compound (Physcion) [85]. High drug loading (11.49%) and encapsulation efficiency (88%) were achieved. In contrast to free Physcion, the antibacterial activity of Physcion@ZIF-8 against gram-positive and gram-negative bacteria is much higher. Therefore, it indicates that loading the Physcion into ZIF-8 is beneficial for drug delivery against many infectious diseases.

Hyaluronic acid (HA) is a natural polysaccharide and

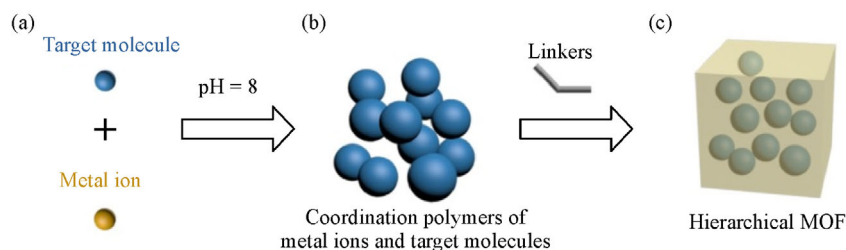


Fig. 7 The pH-induced one-pot synthesis of ZIF-8 to load DOX. Reprinted with permission from ref. [82]. Copyright 2016, American Chemical Society.

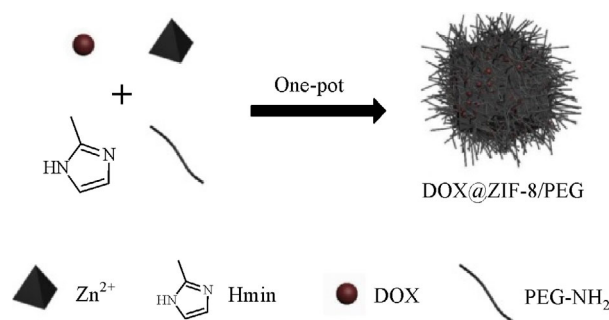


Fig. 8 The preparation of DOX@ZIF-8/PEG via one-pot method. Reprinted with permission from ref. [83]. Copyright 2019, Elsevier.

has exhibited outstanding performance on wound healing [86]. However, its instability and low mechanical strength limit its regular application in this field. HA/ZIF-8 used for wound healing is another good example to demonstrate the application of ZIF-8, as the synthesized HA/ZIF-8 can break the limitation [87]. Due to the hydrogen bonds between HA and ZIF-8 and the high stress transfer property of ZIF-8, HA/ZIF-8 has shown improved mechanical properties. Antibacterial characteristics as well as cell adhesion on HA-modified films are also improved. Therefore, HA film modification by ZIF-8 has brought desirable features for wound healing purposes [88].

Coronas's group encapsulated caffeine, an amphiphilic compound, in ZIF-8 via two strategies [89]. The first method is an *in situ* encapsulation where caffeine is added to a ZIF-8 preparation solution and the ZIF-8 structure is formed around the entrapped molecule. For the second *ex situ* strategy, caffeine is mixed with previously synthesized ZIF-8. The *in situ* one-step encapsulation enables the controlled release of caffeine (during 27 days) and a high drug loading (ca. 28 wt-%), which is better than the *ex situ* method [89]. These features are a result of the van der Waals interactions between ZIF-8 and caffeine [90]. ZIF-8 can encapsulate hydrophobic, hydrophilic and amphiphilic drugs.

3.2 ZIF-8 as nanocarrier for photothermal agents

Photothermal therapy (PTT) is a promising alternative to

traditional cancer treatment and has attracted wide attention due to its non-invasive property [91]. Carbon nanomaterials [92–94], gold nanomaterials [95–97], and metal sulfides [98–100] are typical photothermal agents. However, they are non-biodegradable inorganic materials and have potential long-term toxicity. Therefore, photo-responsive organic dyes that show maximum absorption in the near infrared (NIR) region have been widely used in PTT [101]. Cyanine (Cy) is one of the photothermal agents which exhibit several problems, including fast clearance, poor selectivity and low solubility [102]. Li et al. [103] loaded Cy into ZIF-8 using the one-pot method (Fig. 9). The obtained Cy@ZIF-8 nanoparticles exhibited excellent photo-stability, good water solubility, great photothermal conversion efficiency, and strong NIR absorbance. Remarkably, the Cy@ZIF-8 nanoparticles efficiently inhibited tumor growth effectively *in vivo* and also displayed outstanding NIR imaging capacity [104]. However, in this work, Li et al. applied Cy@ZIF-8 via intratumoral injection, and so there is no information about whether ZIF-8 is toxic to the whole body. Moreover, Cy is released at a slow rate under neutral conditions (pH = 7.4). The premature release should be investigated in more details.

Indocyanine green (ICG) is a dye that has been approved by the United States Food and Drug Administration for optical imaging of human vasculature in NIR [105]. ICG has outstanding photothermal conversion ability for PTT [106]. However, it lacks target specificity, thermal stability, and photo-stability [107]. In order to overcome these

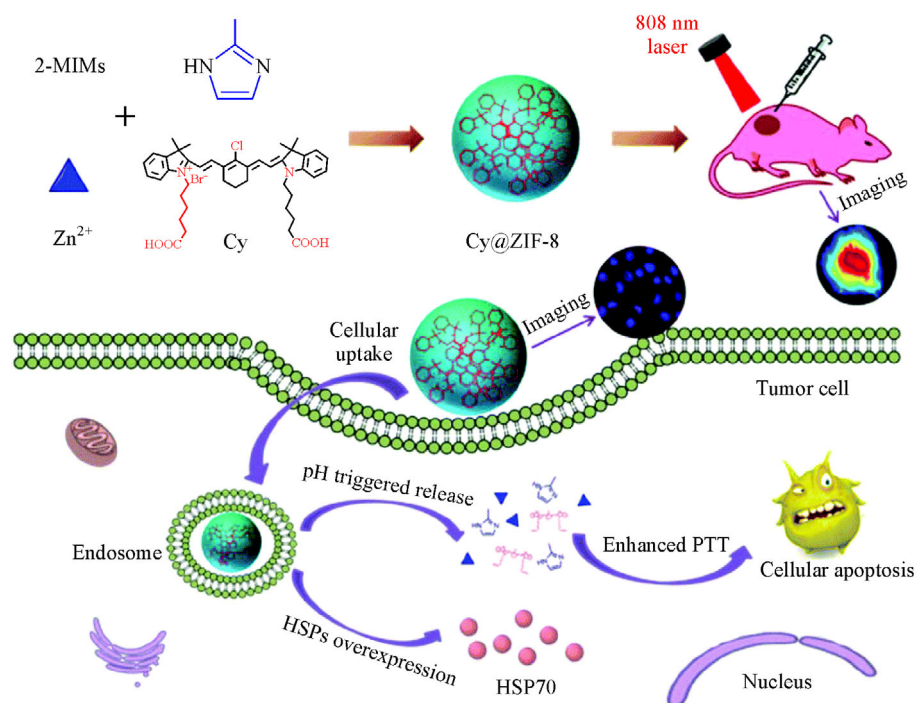


Fig. 9 Synthesis of Cy@ZIF-8 nanoparticles and their application for NIR fluorescent imaging and photothermal therapy. Reprinted with permission from ref. [103]. Copyright 2018, The Royal Society of Chemistry.

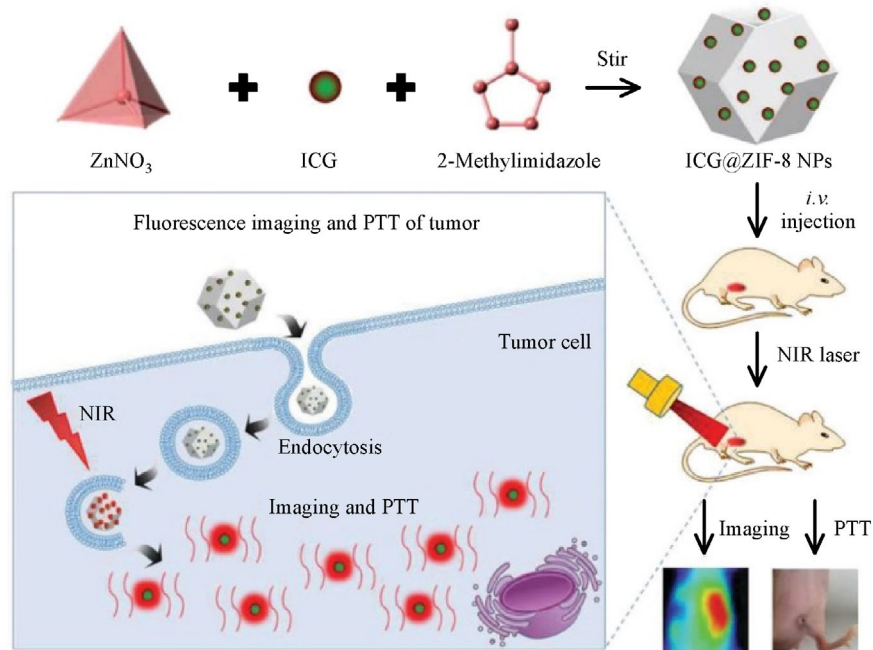


Fig. 10 Schematic illustration of the one-pot synthesis of ICG@ZIF-8 nanoparticles and its application for fluorescence imaging and photothermal therapy of tumor *in vivo*. Reprinted with permission from ref. [108]. Copyright 2018, The Royal Society of Chemistry.

shortcomings, Wang et al. [108] constructed a ZIF-8-based ICG theranostic system for PTT and fluorescence imaging by one-pot method (Fig. 10). The as-synthesized ICG@ZIF-8 nanoparticles show favorable photothermal killing capacity, ultrahigh loading capacity, efficient cellular uptake, superior photothermal stability, and good biocompatibility. More significantly, the *in vivo* experiments revealed that ICG@ZIF-8 nanoparticles could accurately permit the detection of tumors by fluorescence molecular imaging [108]. The Wang group used methanol as the solvent to prepare ICG@ZIF-8 nanoparticles and the organic solvent residue may cause a potential toxicity of ZIF-8 *in vivo*.

3.3 ZIF-8 as nanocarrier for photodynamic agents

Compared to traditional tumor treatments, photodynamic therapy (PDT) for tumor treatment exhibits two significant advantages, e.g., the simultaneous fluorescence imaging and a noninvasive nature. Therefore, it has attracted broad attention in recent years [109,110]. In PDT, the photosensitizer (PS) interacts with available oxygen molecules under the condition of light irradiation [111,112]. However, lots of efficient PSs tend to self-aggregate in aqueous solution due to their hydrophobicity, which will lead to quick quenching of the fluorescence imaging [113]. Xu et al. [114] constructed ZnPc@ZIF-8 to solve these problems (Fig. 11). The hydrophobic ZnPc molecule stored in the pores of ZIF-8 remains at the monomeric state, which prevents self-aggregation. Under light irradiation

at a wavelength of 650 nm, it undergoes photo excitation to convert triplet oxygen ($^3\text{O}_2$) to singlet oxygen ($^1\text{O}_2$) in aqueous medium. Moreover, ZnPc@ZIF-8 can be completely degraded after PDT due to its acid-sensitive property, which also provides a method to monitor its variation through the self-quenching of fluorescence emission of ZnPc [114]. However, the rapid proliferation of tumor cells causes hypoxia in solid tumors. Moreover, the PDT process needs oxygen. Therefore, some O_2 storage materials have been utilized to reduce the hypoxia within tumors. It is noteworthy that the research work was conducted using HepG-2 cells *in vitro*, and further experiments are needed to investigate the performance of the ZnPc@ZIF-8 in the more complicated *in vivo* environment.

A core-shell nanostructure, $\text{O}_2\text{-Cu/ZIF-8@Ce6/ZIF-8}$, was developed to relieve tumor hypoxia to enhance PDT [115]. By a simple ion-doping manner, Cu^{2+} -doped ZIF-8 (Cu/ZIF-8) was prepared in this work. O_2 adsorption isotherms confirmed that the Cu/ZIF-8 possesses enhanced O_2 storage capacity. Then, a thin layer of ZIF-8 containing chlorin e6 (Ce6) was applied to the surface of Cu/ZIF-8. Finally, F127, a highly biocompatible polymer layer, was deposited onto $\text{O}_2\text{-Cu/ZIF-8@Ce6/ZIF-8}$. Upon *in vivo* delivery, Cu^{2+} , Ce6, and O_2 are released under the acidic tumor microenvironment. On one hand, the intratumoral glutathione (GSH) is oxidized by the Cu^{2+} which depletes the content of GSH. Then the generated Cu^+ reacts with H_2O_2 and induces the highly efficient Fenton-like reaction to produce O_2 and $\cdot\text{OH}$. On

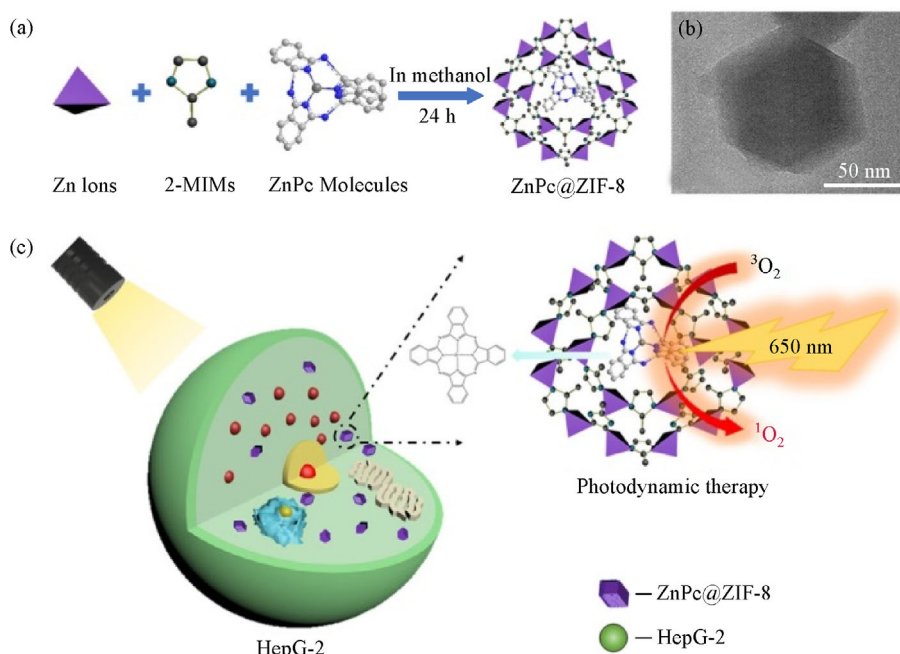


Fig. 11 (a) Fabrication of ZnPc@ZIF-8. (b) TEM Image of ZnPc@ZIF-8. (c) *In vitro* PDT in HepG-2 cells using ZnPc@ZIF-8. Reprinted with permission from ref. [114]. Copyright 2018, American Chemical Society.

the other hand, the produced O_2 relieves tumor hypoxia and enhances the PDT efficacy. This integrated nanocarrier significantly presents high-efficiency enhanced antitumor treatment both *in vitro* and *in vivo*.

3.4 ZIF-8 as nanocarrier for chemodynamic therapy

Chemodynamic therapy (CDT) is a booming cancer treatment modality [116,117]. The iron-based Fenton reaction is used to kill cancer cells by transforming intracellular H_2O_2 to hydroxyl radicals ($\cdot OH$). The endogenous stimuli-responsive $\cdot OH$ generation enables a specific cancer therapy without the need of external energy input. Copper ions and MnO_2 are also used for CDT [117,118]. As the most widespread elements in reactive oxygen species (ROS), $\cdot OH$ and 1O_2 can cause damage to tumor tissues. In addition, ROS-mediated cancer treatment may cause more damage to cancer cells than normal cells because of the different redox states [119].

Traditional singlet oxygen-based antitumor therapies need external energy input, such as ultrasound and light, and can cause detrimental dark toxicity. Ascorbate accumulates hydrogen peroxide only in the tumor tissues at a pharmacological concentration. Simultaneous delivery of ascorbate and nanoparticulate hypochlorous ions (ClO^-) produces singlet oxygen at the tumor site, which is an energy-free and tumor-specific treatment. Chen et al. [120] prepared the $NaClO@ZIF-8@Pluronic\ F68$ nanocarrier by one-pot method as shown in Fig. 12. By the synergistic effect of the nanocarrier and the ascorbic acid, the

production of intracellular singlet oxygen was confirmed in 4T1 cells, which induced significant apoptotic cell death. After intravenous administration of nanocarriers to xenograft mice and intraperitoneal administration of ascorbic acid, the *in vivo* antitumor efficacy of this synergistic nanomedicine was proven to have no significant side effects. This work demonstrates the singlet oxygen-based chemodynamic therapy for eradication of selective tumors, which constitutes a non-triggered, singlet oxygen-based cancer therapy without traditional photodynamic and sonodynamic therapy side effects. The drug loading in this work is just $(6.1 \pm 0.3)\%$ (w/w). This may be attributed to the leakage of $NaClO$ through the pores of ZIF-8 during the preparation process. If the preparation process can be optimized to avoid $NaClO$ leakage, there will be a positive impact on its utilization in drug delivery.

3.5 ZIF-8 as nanocarrier for protein

Protein therapeutics have received wide attention because of their high potency [121,122]. However, many proteins are unstable and their properties (including conformation) are influenced by temperature and pH [123,124]. These shortcomings limit the usage of proteins for therapy usage. MOFs encapsulation has been used to stabilize proteins via providing structural and chemical protection [125–127]. It was proven that encapsulating proteins in ZIF-8 can protect these proteins against conformational changes under adverse conditions [126].

Smart glucose-responsive vehicles have been used in the

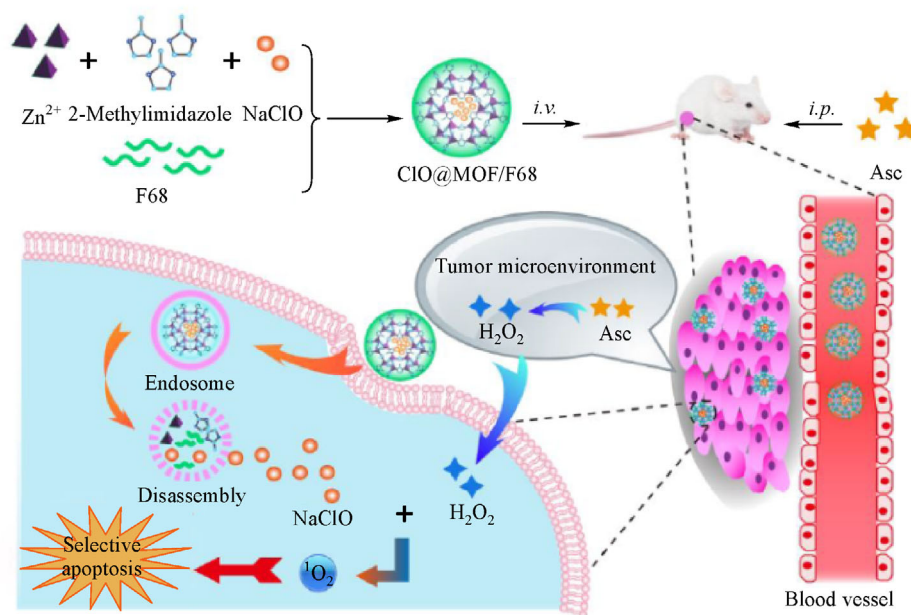


Fig. 12 Illustration of 1O_2 -based CDT that was realized by intravenous (*i.v.*) delivery of hybrid nanocarrier ($ClO@MOF/F68$) and concurrent intraperitoneal (*i.p.*) administration of ascorbate (Asc). Reprinted with permission from ref. [120]. Copyright 2019, John Wiley and Sons.

therapy of diabetic patients [128–130]. Chen et al. [131] loaded the enzyme glucose oxidase (GOx) into ZIF-8 materials. Specially, the GOx was encapsulated into the ZIF-8 via one-pot method with modified insulin. GOx is an enzyme that can oxidize glucose to gluconic acid, which is accompanied by the production of hydrogen peroxide. Then, the glucose-responsive vehicles released GOx due to destruction of ZIF-8 at low pH. Therefore, the GOx-loaded ZIF-8 was used as smart vehicles for treating diabetes or macular diseases [131].

Hemoglobin as a natural protein in red blood cells is responsible for transporting oxygen in the blood vessels of vertebrates [132]. Hemoglobin and GOx were both encapsulated by a co-precipitation procedure into pH-sensitive ZIF-8 [133]. Firstly, the hemoglobin (50 mg in 1 mL) and GOx (50 mg in 1 mL) stock solutions were added to a solution of MIM (25 mmol) in ultra-pure water (20 mL) (Fig. 13). The mixed solutions were stirred at room temperature for 15 min, then a solution of Zn (NO_3)₂·6H₂O (185 mg, 0.62 mmol) in ultra-pure water (2 mL) was added, and the mixture was stirred for 30 min. It was reported that the GOx&Hb@ZIF-8 was steady at pH 7.4 and did not present any activity. It was activated and destroyed at lower pH to produce high levels of reactive hydroxyl radicals ($\cdot\text{OH}$). This is a pioneer research using the pH-sensitive ZIF-8 to deliver hemoglobin and GOx for the effective tumor therapy following combined starvation and Fenton therapies [133]. However, the blank ZIF-8 was not used *in vitro* studies and its toxic effects are not evaluated under the *in vitro* condition. Moreover, the systemic toxicity and degradation of GOx&Hb@ZIF-8 *in vivo* need further investigation.

3.6 ZIF-8 as nanocarrier for genome editing

CRISPR/Cas9 is a famous genome editing tool to provide fundamental and revolutionary solutions for genetic diseases. It combines the manipulation of the engineered single guide RNA (sgRNA) and the protein Cas9 [134]. However, it has a double delivery problem due to the highly charged RNA module and the large protein size [135]. As outlined above, ZIF-8 has a distinctive pH-sensitive ability, which exhibits the potential to escape the

endocytic pathway [136]. The first case of CRISPR/Cas9 encapsulated in ZIF-8 was reported by Alsaiari et al. [127], as shown in Fig. 14. CRISPR/Cas9@ZIF-8 were prepared via the following procedures: Equal amounts of sgRNA and Cas9 were mixed, and then the MIM solution was added to the mixture. Finally, an aqueous solution of zinc nitrate was added under mechanical agitation at room temperature until the clear solution became opaque. It was found that the nanoscale CRISPR/Cas9@ZIF-8 exhibits excellent loading capacity and can be used to control the codelivery of sgRNA and Cas9 protein. In addition, this material is biocompatible and can also be produced at large scale. ZIF-8 can protect both the negatively charged sgRNA and the large Cas9 protein within a high loading ability of 1.2% (w/w). In this process, it is essential for genetic transfection to achieve the protonation of the imidazole-based framework at the endosomal pH, which facilitates enhanced nuclei delivery and fast endosomal escape. Therefore, this scheme provides an efficient method for the delivery of CRISPR/Cas9 for gene editing [127]. This work is mainly concerned about the role of CRISPR/Cas9@ZIF-8 in the treatment of genetic diseases. The effect of the toxicity of CRISPR/Cas9@ZIF-8 needs to be studied, which is undoubtedly very important for future applications.

4 Potential risks of ZIF-8 in drug delivery

ZIF-8 materials have been successfully used in the applications of drug delivery due to their unique advantages. The efficient delivery of various kinds of drugs using ZIF-8 as nanocarrier has been reported. However, there are several potential risks and challenges to be addressed before clinical applications of these materials become feasible: (1) For biomedical and pharmaceutical applications, ZIF-8 materials need to be biocompatible. However, ZIF-8 is composed of Zn ions and MIM. Their toxicities are characterized by the oral median lethal dose 50 (LD₅₀), i.e., 350 $\mu\text{g}\cdot\text{kg}^{-1}$ for Zn and 1.13 $\text{g}\cdot\text{kg}^{-1}$ for MIM. Therefore, the toxicity of ZIF-8 cannot be ignored based on the reported LD₅₀ of both components. The usage of ZIF-8 *in vivo* as part of a

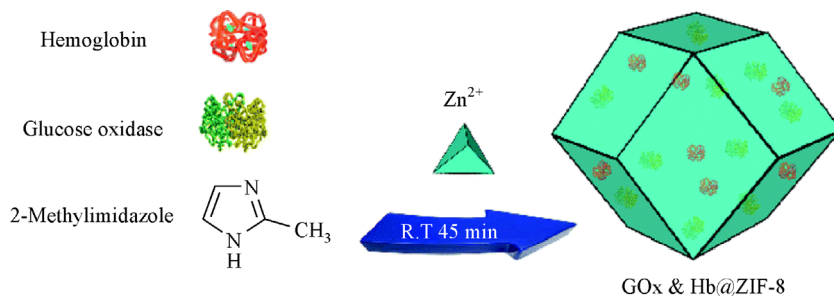


Fig. 13 Schematic illustration of the preparation of GOx&Hb@ZIF-8. Reprinted with permission from ref. [133]. Copyright 2019, The Royal Society of Chemistry.

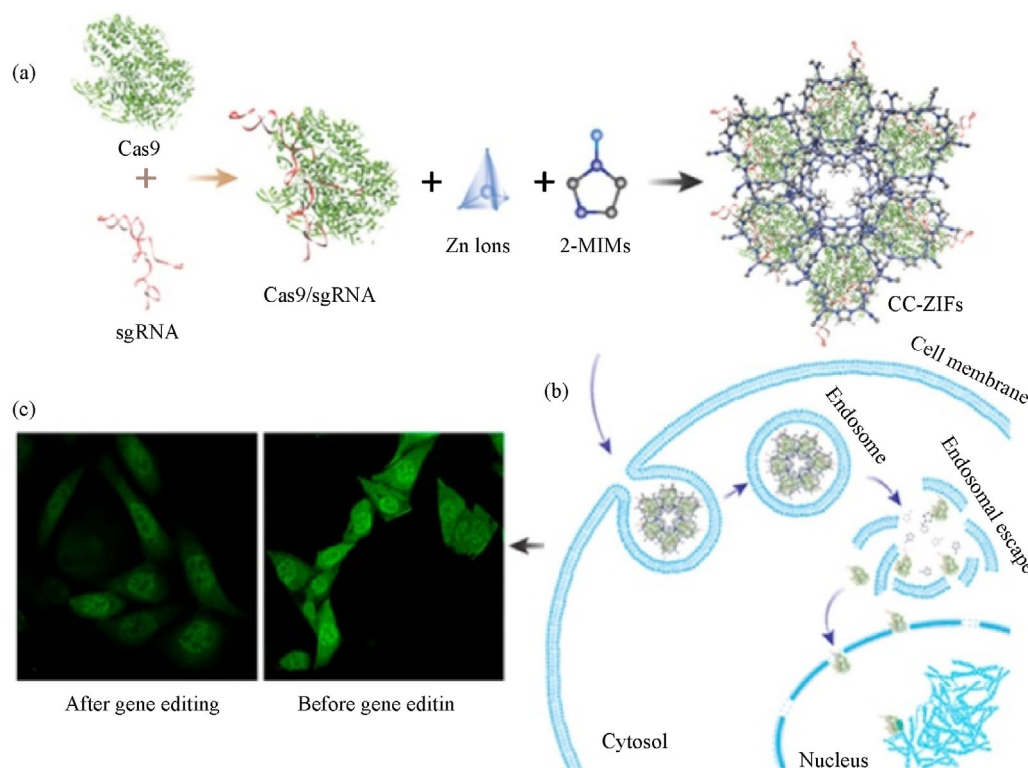


Fig. 14 (a) The encapsulation of the Cas9/sgRNA in ZIF-8 to prepare CC-ZIFs. (b) Endosomal escape of CC-ZIFs. (c) CLSM images of cells before and after treatment with CC-ZIFs. Reprinted with permission from ref. [127]. Copyright 2018, American Chemical Society.

pharmacological treatment implies active uptake of Zn into the organism. In this case, the exposure of the organism to Zn ions is determined by the intensity (dose), frequency, and duration of the treatment. The treatment route also influences the distribution, metabolism and elimination of Zn ions in the organism. The LD_{50} value for one treatment route may be not applicable for other routes due to different biodistributions. Moreover, when considering the toxicity of ZIF-8 in the human body, there is even less data available for MIM ligands. In addition to the toxicity associated with the ZIF-8 itself, toxicity issues can also be closely related to the synthesis processes, especially those including the use of solvents such as DMF and reaction modulators for the preparation of NPs. The solvent residue may pose a potential toxicity issue. Thus, to prepare suitable nanomaterials for clinical applications, alternative green synthesis routes are urgently needed. (2) Biodegradability is a vital aspect and one of the most intriguing advantages for the biomedical applications of ZIF-8. ZIF-8 possesses intrinsic biodegradability due to the reversible coordination between Zn ions and MIM ligands. At low pH conditions, ZIF-8 can decompose to enable the rapid release of loaded drugs. The drug release kinetics will definitely affect the drug efficacy and therapy outcome. The degradation mechanisms and degradation products of ZIF-8 under physiological conditions are so far unclear. Some previous work reported that certain MOFs became amorphous and underwent structural rearrangements and/

or reactions that generated new inorganic species upon contacting with cell culture medium. Thus, the *in vivo* biodegradability of ZIF-8 still needs more investigation.

5 Conclusions and outlook

Extensive research effort has been devoted to the synthesis and drug delivery applications of ZIF-8 and promising progress in both aspects has been achieved in recent years.

Several synthesis methods, including traditional and non-traditional approaches, have been developed to produce ZIF-8 materials with different forms and properties. The traditional strategies including solvothermal and hydrothermal methods have been broadly used to prepare ZIF-8. Furthermore, the sonochemical and mechanochemical synthesis methods have also been proposed to overcome the limitations of the traditional strategies. Moreover, the accelerated aging method has been developed and used for the synthesis of ZIF-8. In general, the synthesis methods determine the properties of ZIF-8.

The unique molecular structure and properties of ZIF-8 make it a unique vehicle in drug delivery. Generally, ZIF-8 shows good dispersity, high loading capacity, high thermal and chemical stabilities, and pH-sensitive degradation. Based on these excellent properties, ZIF-8 is widely used as the nanocarrier for the delivery of chemical drugs, photothermal agents, photodynamic agents, chemodynamic

agents, nucleic acid therapeutics, RNA-protein CRISPR complexes, and proteins. There are several potential risks and challenges regarding ZIF-8. The toxicity of the nanocarrier is a main obstacle. The degradation mechanism and degradation products of ZIF-8 under physiological conditions need more investigation.

In order to develop new synthesis methods and to discover the novel attractive drug delivery applications of ZIF-8, it is important to make use of the experience and knowledge obtained from related areas, for example in the inorganic materials. ZIF-8 has gained broad attention and tremendous achievement has been made in recent years. We believe that new techniques and concepts for synthesis and utilization of the fast growing field of ZIF-8 materials will continue to develop in the near future.

Acknowledgements SMF and ZW acknowledge the financial support from the Natural Science Foundation of Tianjin (No. 19JCYBJC28400). XLZ and DYS acknowledge the funding support from the Basic Research General Program of Shenzhen Science and Technology Innovation Commission in 2020.

References

- Cheetham A K, Rao C N, Feller R K. Structural diversity and chemical trends in hybrid inorganic-organic framework materials. *Chemical Communications*, 2006, (46): 4780–4795
- Li J R, Kuppler R J, Zhou H C. Selective gas adsorption and separation in metal-organic frameworks. *Chemical Society Reviews*, 2009, 38(5): 1477–1504
- Ferey G, Mellot-Draznieks C, Serre C, Millange F. Crystallized frameworks with giant pores: Are there limits to the possible? *Accounts of Chemical Research*, 2005, 38(4): 217–225
- O’Keeffe M, Peskov M A, Ramsden S J, Yaghi O M. The reticular chemistry structure resource (RCSR) database of, and symbols for, crystal nets. *Accounts of Chemical Research*, 2008, 41(12): 1782–1789
- Banerjee R, Phan A, Wang B, Knobler C, Furukawa H, O’Keeffe M, Yaghi O M. High-throughput synthesis of zeolitic imidazolate frameworks and application to CO₂ capture. *Science*, 2008, 319(5865): 939–943
- Moggach S A, Bennett T D, Cheetham A K. The effect of pressure on zif-8: Increasing pore size with pressure and the formation of a high-pressure phase at 1.47 gpa. *Angewandte Chemie International Edition*, 2009, 48(38): 7087–7089
- Fairen-Jimenez D, Moggach S A, Wharmby M T, Wright P A, Parsons S, Duren T. Opening the gate: Framework flexibility in ZIF-8 explored by experiments and simulations. *Journal of the American Chemical Society*, 2011, 133(23): 8900–8902
- Wang F, Tan Y X, Yang H, Zhang H X, Kang Y, Zhang J. A new approach towards tetrahedral imidazolate frameworks for high and selective CO₂ uptake. *Chemical Communications*, 2011, 47(20): 5828–5830
- Li Y, Liang F, Bux H, Yang W, Caro J. Zeolitic imidazolate framework ZIF-7 based molecular sieve membrane for hydrogen separation. *Journal of Membrane Science*, 2010, 354(1-2): 48–54
- Liu Y, Hu E, Khan E A, Lai Z. Synthesis and characterization of ZIF-69 membranes and separation for CO₂/CO mixture. *Journal of Membrane Science*, 2010, 353(1-2): 36–40
- McCarthy M C, Varela-Guerrero V, Barnett G V, Jeong H K. Synthesis of zeolitic imidazolate framework films and membranes with controlled microstructures. *Langmuir*, 2010, 26(18): 14636–14641
- Jiang H L, Liu B, Akita T, Haruta M, Sakurai H, Xu Q. Au@ZIF-8: CO oxidation over gold nanoparticles deposited to metal-organic framework. *Journal of the American Chemical Society*, 2009, 131(32): 11302–11303
- Chizallet C, Lazare S, Bazer-Bachi D, Bonnier F, Lecocq V, Soyer E, Quoineaud A A, Bats N. Catalysis of transesterification by a nonfunctionalized metal-organic framework: Acido-basicity at the external surface of ZIF-8 probed by FTIR and *ab initio* calculations. *Journal of the American Chemical Society*, 2010, 132(35): 12365–12377
- Wu H, Zhou W, Yildirim T. Hydrogen storage in a prototypical zeolitic imidazolate framework-8. *Journal of the American Chemical Society*, 2007, 129(17): 5314–5315
- Murray L J, Dinca M, Long J R. Hydrogen storage in metal-organic frameworks. *Chemical Society Reviews*, 2009, 38(5): 1294–1314
- Ma S, Zhou H C. Gas storage in porous metal-organic frameworks for clean energy applications. *Chemical Communications*, 2010, 46(1): 44–53
- Harbuzaru B V, Corma A, Rey F, Jorda J L, Ananias D, Carlos L D, Rocha J. A miniaturized linear pH sensor based on a highly photoluminescent self-assembled europium(III) metal-organic framework. *Angewandte Chemie International Edition*, 2009, 48(35): 6476–6479
- Lu G, Hupp J T. Metal-organic frameworks as sensors: A ZIF-8 based fabry-perot device as a selective sensor for chemical vapors and gases. *Journal of the American Chemical Society*, 2010, 132(23): 7832–7833
- Lu D, An Y, Feng S, Li X, Fan A, Wang Z, Zhao Y. Imidazole-bearing polymeric micelles for enhanced cellular uptake, rapid endosomal escape, and on-demand cargo release. *AAPS PharmSciTech*, 2018, 19(6): 2610–2619
- Li X, Gao M, Xin K, Zhang L, Ding D, Kong D, Wang Z, Shi Y, Kiessling F, Lammers T, Cheng J, Zhao Y. Singlet oxygen-responsive micelles for enhanced photodynamic therapy. *Journal of Controlled Release*, 2017, 260: 12–21
- Li J, Meng X, Deng J, Lu D, Zhang X, Chen Y, Zhu J, Fan A, Ding D, Kong D, Wang Z, Zhao Y. Multifunctional micelles dually responsive to hypoxia and singlet oxygen: Enhanced photodynamic therapy via interactively triggered photosensitizer delivery. *ACS Applied Materials & Interfaces*, 2018, 10(20): 17117–17128
- Meng X, Deng J, Liu F, Guo T, Liu M, Dai P, Fan A, Wang Z, Zhao Y. Triggered all-active metal organic framework: Ferroptosis machinery contributes to the apoptotic photodynamic antitumor therapy. *Nano Letters*, 2019, 19(11): 7866–7876

23. Park K S, Ni Z, Cote A P, Choi J Y, Huang R, Uribe-Romo F J, Chae H K, O'Keeffe M, Yaghi O M. Exceptional chemical and thermal stability of zeolitic imidazolate frameworks. *Proceedings of the National Academy of Sciences of the United States of America*, 2006, 103(27): 10186–10191
24. Rohani S, Isimjan T, Mohamed A, Kazemian H, Salem M, Wang T. Fabrication, modification and environmental applications of TiO₂ nanotube arrays (TNTAs) and nanoparticles. *Frontiers of Chemical Science and Engineering*, 2011, 6(1): 112–122
25. Kida K, Okita M, Fujita K, Tanaka S, Miyake Y. Formation of high crystalline ZIF-8 in an aqueous solution. *CrystEngComm*, 2013, 15(9): 1794
26. Huang X C, Lin Y Y, Zhang J P, Chen X M. Ligand-directed strategy for zeolite-type metal-organic frameworks: Zinc(II) imidazolates with unusual zeolitic topologies. *Angewandte Chemie International Edition*, 2006, 45(10): 1557–1559
27. Zhang J P, Zhu A X, Lin R B, Qi X L, Chen X M. Pore surface tailored sod-type metal-organic zeolites. *Advanced Materials*, 2011, 23(10): 1268–1271
28. Zhu A X, Lin R B, Qi X L, Liu Y, Lin Y Y, Zhang J P, Chen X M. Zeolitic metal azolate frameworks (MAFs) from ZnO/Zn(OH)₂ and monoalkyl-substituted imidazoles and 1,2,4-triazoles: Efficient syntheses and properties. *Microporous and Mesoporous Materials*, 2012, 157: 42–49
29. Cravillon J, Münzer S, Lohmeier S J, Feldhoff A, Huber K, Wiebcke M. Rapid room-temperature synthesis and characterization of nanocrystals of a prototypical zeolitic imidazolate framework. *Chemistry of Materials*, 2009, 21(8): 1410–1412
30. Cravillon J, Nayuk R, Springer S, Feldhoff A, Huber K, Wiebcke M. Controlling zeolitic imidazolate framework nano- and micro-crystal formation: Insight into crystal growth by time-resolved *in situ* static light scattering. *Chemistry of Materials*, 2011, 23(8): 2130–2141
31. Cravillon J, Schröder C A, Bux H, Rothkirch A, Caro J, Wiebcke M. Formate modulated solvothermal synthesis of ZIF-8 investigated using time-resolved *in situ* X-ray diffraction and scanning electron microscopy. *CrystEngComm*, 2012, 14(2): 492–498
32. Nune S K, Thallapally P K, Dohnalkova A, Wang C, Liu J, Exarhos G J. Synthesis and properties of nano zeolitic imidazolate frameworks. *Chemical Communications*, 2010, 46(27): 4878–4880
33. Bennett T D, Saines P J, Keen D A, Tan J C, Cheetham A K. Ball-milling-induced amorphization of zeolitic imidazolate frameworks (ZIFs) for the irreversible trapping of iodine. *Chemistry (Weinheim an der Bergstrasse, Germany)*, 2013, 19(22): 7049–7055
34. He M, Yao J, Li L, Wang K, Chen F, Wang H. Synthesis of zeolitic imidazolate framework-7 in a water/ethanol mixture and its ethanol-induced reversible phase transition. *ChemPlusChem*, 2013, 78(10): 1222–1225
35. Shen K, Zhang L, Chen X, Liu L, Zhang D, Han Y, Chen J, Long J, Luque R, Li Y, Chen B. Ordered macro-microporous metal-organic framework single crystals. *Science*, 2018, 359(6372): 206–210
36. Hu L, Yan Z, Zhang J, Peng X, Mo X, Wang A, Chen L. Surfactant aggregates within deep eutectic solvent-assisted synthesis of hierarchical ZIF-8 with tunable porosity and enhanced catalytic activity. *Journal of Materials Science*, 2019, 54(16): 11009–11023
37. Chen Y, Tang S. Solvothermal synthesis of porous hydrangea-like zeolitic imidazole framework-8 (ZIF-8) crystals. *Journal of Solid State Chemistry*, 2019, 276: 68–74
38. Troyano J, Carne-Sanchez A, Avci C, Imaz I, Maspocho D. Colloidal metal-organic framework particles: The pioneering case of ZIF-8. *Chemical Society Reviews*, 2019, 48(23): 5534–5546
39. Pan Y, Liu Y, Zeng G, Zhao L, Lai Z. Rapid synthesis of zeolitic imidazolate framework-8 (ZIF-8) nanocrystals in an aqueous system. *Chemical Communications*, 2011, 47(7): 2071–2073
40. Tanaka S, Kida K, Okita M, Ito Y, Miyake Y. Size-controlled synthesis of zeolitic imidazolate framework-8 (ZIF-8) crystals in an aqueous system at room temperature. *Chemistry Letters*, 2012, 41(10): 1337–1339
41. Gross A F, Sherman E, Vajo J J. Aqueous room temperature synthesis of cobalt and zinc sodalite zeolitic imidazolate frameworks. *Dalton Transactions (Cambridge, England)*, 2012, 41(18): 5458–5460
42. Yao J, He M, Wang K, Chen R, Zhong Z, Wang H. High-yield synthesis of zeolitic imidazolate frameworks from stoichiometric metal and ligand precursor aqueous solutions at room temperature. *CrystEngComm*, 2013, 15(18): 3601
43. He M, Yao J, Liu Q, Wang K, Chen F, Wang H. Facile synthesis of zeolitic imidazolate framework-8 from a concentrated aqueous solution. *Microporous and Mesoporous Materials*, 2014, 184: 55–60
44. Seoane B, Zamaro J M, Tellez C, Coronas J. Sonocrystallization of zeolitic imidazolate frameworks (ZIF-7, ZIF-8, ZIF-11 and ZIF-20). *CrystEngComm*, 2012, 14(9): 3103
45. Cho H Y, Kim J, Kim S N, Ahn W S. High yield 1-L scale synthesis of ZIF-8 via a sonochemical route. *Microporous and Mesoporous Materials*, 2013, 169: 180–184
46. Suslick K S, Hammerton D A, Cline R E. Sonochemical hot spot. *Journal of the American Chemical Society*, 1986, 108(18): 5641–5642
47. Son W J, Kim J, Kim J, Ahn W S. Sonochemical synthesis of MOF-5. *Chemical Communications*, 2008, (47): 6336–6338
48. Schlesinger M, Schulze S, Hietschold M, Mehring M. Evaluation of synthetic methods for microporous metal-organic frameworks exemplified by the competitive formation of [Cu₂(btc)₃(H₂O)₃] and. *Microporous and Mesoporous Materials*, 2010, 132(1-2): 121–127
49. Fernández-Bertrán J F, Hernández M P, Reguera E, Yee-Madeira H, Rodriguez J, Paneque A, Llopiz J C. Characterization of mechanochemically synthesized imidazolates of Ag⁺¹, Zn⁺², Cd⁺², and Hg⁺²: Solid state reactivity of nd¹⁰ cations. *Journal of Physics and Chemistry of Solids*, 2006, 67(8): 1612–1617
50. Adams C J, Colquhoun H M, Crawford P C, Lusi M, Orpen A G. Solid-state interconversions of coordination networks and hydrogen-bonded salts. *Angewandte Chemie International Edition*, 2007, 119(7): 1142–1146
51. Beldon P J, Fabian L, Stein R S, Thirumurugan A, Cheetham A K, Friscic T. Rapid room-temperature synthesis of zeolitic imidazo-

- late frameworks by using mechanochemistry. *Angewandte Chemie International Edition*, 2010, 49(50): 9640–9643
52. Braga D, Curzi M, Johansson A, Polito M, Rubini K, Grepioni F. Simple and quantitative mechanochemical preparation of a porous crystalline material based on a 1D coordination network for uptake of small molecules. *Angewandte Chemie International Edition*, 2006, 45(1): 142–146
53. Friscic T, Reid D G, Halasz I, Stein R S, Dinnebier R E, Duer M J. Ion- and liquid-assisted grinding: Improved mechanochemical synthesis of metal-organic frameworks reveals salt inclusion and anion templating. *Angewandte Chemie International Edition*, 2010, 49(4): 712–715
54. Tanaka S, Kida K, Nagaoka T, Ota T, Miyake Y. Mechanochemical dry conversion of zinc oxide to zeolitic imidazolate framework. *Chemical Communications*, 2013, 49(72): 7884–7886
55. Cao S, Bennett T D, Keen D A, Goodwin A L, Cheetham A K. Amorphization of the prototypical zeolitic imidazolate framework ZIF-8 by ball-milling. *Chemical Communications*, 2012, 48(63): 7805–7807
56. Lewis D W, Ruiz-Salvador A R, Gómez A, Rodriguez-Albelo L M, Coudert F X, Slater B, Cheetham A K, Mellot-Draznieks C. Zeolitic imidazole frameworks: Structural and energetics trends compared with their zeolite analogues. *CrystEngComm*, 2009, 11(11): 2272
57. Tan J C, Cheetham A K. Mechanical properties of hybrid inorganic-organic framework materials: Establishing fundamental structure-property relationships. *Chemical Society Reviews*, 2011, 40(2): 1059–1080
58. Tan J C, Bennett T D, Cheetham A K. Chemical structure, network topology, and porosity effects on the mechanical properties of zeolitic imidazolate frameworks. *Proceedings of the National Academy of Sciences of the United States of America*, 2010, 107(22): 9938–9943
59. Cliffe M J, Mottillo C, Stein R S, Bučar D K, Friščić T. Accelerated aging: A low energy, solvent-free alternative to solvothermal and mechanochemical synthesis of metal-organic materials. *Chemical Science (Cambridge)*, 2012, 3(8): 2495
60. Mottillo C, Lu Y, Pham M H, Cliffe M J, Do T O, Friščić T. Mineral neogenesis as an inspiration for mild, solvent-free synthesis of bulk microporous metal-organic frameworks from metal (Zn, Co) oxides. *Green Chemistry*, 2013, 15(8): 2121
61. Lee J, Farha O K, Roberts J, Scheidt K A, Nguyen S T, Hupp J T. Metal-organic framework materials as catalysts. *Chemical Society Reviews*, 2009, 38(5): 1450–1459
62. Xiao D J, Bloch E D, Mason J A, Queen W L, Hudson M R, Planas N, Borycz J, Dzubak A L, Verma P, Lee K, Bonino F, Crocellà V, Yano J, Bordiga S, Truhlar D G, Gagliardi L, Brown C M, Long J R. Oxidation of ethane to ethanol by N₂O in a metal-organic framework with coordinatively unsaturated iron(II) sites. *Nature Chemistry*, 2014, 6(7): 590–595
63. Nguyen L T L, Le K K A, Truong H X, Phan N T S. Metal-organic frameworks for catalysis: The knoevenagel reaction using zeolite imidazolate framework ZIF-9 as an efficient heterogeneous catalyst. *Catalysis Science & Technology*, 2012, 2(3): 521–528
64. Tran U P N, Le K K A, Phan N T S. Expanding applications of metal-organic frameworks: Zeolite imidazolate framework ZIF-8 as an efficient heterogeneous catalyst for the knoevenagel reaction. *ACS Catalysis*, 2011, 1(2): 120–127
65. Hu Y, Zheng S, Zhang F. Fabrication of MIL-100(Fe)@SiO₂@Fe₃O₄ core-shell microspheres as a magnetically recyclable solid acidic catalyst for the acetalization of benzaldehyde and glycol. *Frontiers of Chemical Science and Engineering*, 2016, 10(4): 534–541
66. Farha O K, Yazaydin A O, Eryazici I, Malliakas C D, Hauser B G, Kanatzidis M G, Nguyen S T, Snurr R Q, Hupp J T. *De novo* synthesis of a metal-organic framework material featuring ultrahigh surface area and gas storage capacities. *Nature Chemistry*, 2010, 2(11): 944–948
67. Rosi N L, Eckert J, Eddaoudi M, Vodak D T, Kim J, O’Keeffe M, Yaghi O M. Hydrogen storage in microporous metal-organic frameworks. *Science*, 2003, 300(5622): 1127–1129
68. Yang S, Lin X, Lewis W, Suyetin M, Bichoutskaia E, Parker J E, Tang C C, Allan D R, Rizkallah P J, Hubberstey P, Champness N R, Mark Thomas K, Blake A J, Schröder M. A partially interpenetrated metal-organic framework for selective hysteretic sorption of carbon dioxide. *Nature Materials*, 2012, 11(8): 710–716
69. Al-Janabi N, Alfutimie A, Siperstein F R, Fan X. Underlying mechanism of the hydrothermal instability of Cu₃(BTC)₂ metal-organic framework. *Frontiers of Chemical Science and Engineering*, 2016, 10(1): 103–107
70. Wang Y, Li C, Meng F, Lv S, Guo J, Liu X, Wang C, Ma Z. CuAlCl₄ doped MIL-101 as a high capacity CO adsorbent with selectivity over N₂. *Frontiers of Chemical Science and Engineering*, 2014, 8(3): 340–345
71. Ma W, Jiang Q, Yu P, Yang L, Mao L. Zeolitic imidazolate framework-based electrochemical biosensor for *in vivo* electrochemical measurements. *Analytical Chemistry*, 2013, 85(15): 7550–7557
72. Liu S, Xiang Z, Hu Z, Zheng X, Cao D. Zeolitic imidazolate framework-8 as a luminescent material for the sensing of metal ions and small molecules. *Journal of Materials Chemistry*, 2011, 21(18): 6649
73. Liu S, Wang L, Tian J, Luo Y, Chang G, Asiri A M, Al-Youbi A O, Sun X. Application of zeolitic imidazolate framework-8 nanoparticles for the fluorescence-enhanced detection of nucleic acids. *ChemPlusChem*, 2012, 77(1): 23–26
74. Ojha R P, Lemieux P A, Dixon P K, Liu A J, Durian D J. Statistical mechanics of a gas-fluidized particle. *Nature*, 2004, 427(6974): 521–523
75. Ferey G, Mellot-Draznieks C, Serre C, Millange F, Dutour J, Surble S, Margiolaki I. A chromium terephthalate-based solid with unusually large pore volumes and surface area. *Science*, 2005, 309(5743): 2040–2042
76. Eddaoudi M, Moler D B, Li H, Chen B, Reineke T M, O’Keeffe M, Yaghi O M. Modular chemistry: Secondary building units as a basis for the design of highly porous and robust metal-organic carboxylate frameworks. *Accounts of Chemical Research*, 2001, 34(4): 319–330
77. Chen B, Xiang S, Qian G. Metal-organic frameworks with

- functional pores for recognition of small molecules. *Accounts of Chemical Research*, 2010, 43(8): 1115–1124
78. Sun C Y, Qin C, Wang X L, Yang G S, Shao K Z, Lan Y Q, Su Z M, Huang P, Wang C G, Wang E B. Zeolitic imidazolate framework-8 as efficient pH-sensitive drug delivery vehicle. *Dalton Transactions (Cambridge, England)*, 2012, 41(23): 6906–6909
79. Lu G, Li S, Guo Z, Farha O K, Hauser B G, Qi X, Wang Y, Wang X, Han S, Liu X, et al. Imparting functionality to a metal-organic framework material by controlled nanoparticle encapsulation. *Nature Chemistry*, 2012, 4(4): 310–316
80. Venna S R, Jasinski J B, Carreon M A. Structural evolution of zeolitic imidazolate framework-8. *Journal of the American Chemical Society*, 2010, 132(51): 18030–18033
81. Broadley M R, White P J, Hammond J P, Zelko I, Lux A. Zinc in plants. *New Phytologist*, 2007, 173(4): 677–702
82. Zheng H, Zhang Y, Liu L, Wan W, Guo P, Nystrom A M, Zou X. One-pot synthesis of metal-organic frameworks with encapsulated target molecules and their applications for controlled drug delivery. *Journal of the American Chemical Society*, 2016, 138(3): 962–968
83. Wang H, Li T, Li J, Tong W, Gao C. One-pot synthesis of poly(ethylene glycol) modified zeolitic imidazolate framework-8 nanoparticles: Size control, surface modification and drug encapsulation. *Colloids and Surfaces. A, Physicochemical and Engineering Aspects*, 2019, 568: 224–230
84. Horcajada P, Chalati T, Serre C, Gillet B, Sebie C, Baati T, Eubank J F, Heurtaux D, Clayette P, Kreuz C, et al. Porous metal-organic-framework nanoscale carriers as a potential platform for drug delivery and imaging. *Nature Materials*, 2010, 9(2): 172–178
85. Soomro N A, Wu Q, Amur S A, Liang H, Ur Rahman A, Yuan Q, Wei Y. Natural drug physcion encapsulated zeolitic imidazolate framework, and their application as antimicrobial agent. *Colloids and Surfaces. B, Biointerfaces*, 2019, 182: 110364
86. Almeida P V, Shahbazi M A, Makila E, Kaasalainen M, Salonen J, Hirvonen J, Santos H A. Amine-modified hyaluronic acid-functionalized porous silicon nanoparticles for targeting breast cancer tumors. *Nanoscale*, 2014, 6(17): 10377–10387
87. Abednejad A, Ghaee A, Nourmohammadi J, Mehrizi A A. Hyaluronic acid/carboxylated zeolitic imidazolate framework film with improved mechanical and antibacterial properties. *Carbohydrate Polymers*, 2019, 222: 115033
88. Shu F, Lv D, Song X L, Huang B, Wang C, Yu Y, Zhao S C. Fabrication of a hyaluronic acid conjugated metal organic framework for targeted drug delivery and magnetic resonance imaging. *RSC Advances*, 2018, 8(12): 6581–6589
89. Liedana N, Galve A, Rubio C, Tellez C, Coronas J. CAF@ZIF-8: One-step encapsulation of caffeine in MOF. *ACS Applied Materials & Interfaces*, 2012, 4(9): 5016–5021
90. de Matas M, Edwards H G M, Lawson E E, Shields L, York P. Ft-Raman spectroscopic investigation of a pseudopolymorphic transition in caffeine hydrate. *Journal of Molecular Structure*, 1998, 440(1-3): 97–104
91. Chu C, Lin H, Liu H, Wang X, Wang J, Zhang P, Gao H, Huang C, Zeng Y, Tan Y, Liu G, Chen X. Tumor microenvironment-triggered supramolecular system as an *in situ* nanotheranostic generator for cancer phototherapy. *Advanced Materials*, 2017, 29(23): 1605928
92. Robinson J T, Welsher K, Tabakman S M, Sherlock S P, Wang H, Luong R, Dai H. High performance *in vivo* near-IR (> 1 μm) imaging and photothermal cancer therapy with carbon nanotubes. *Nano Research*, 2010, 3(11): 779–793
93. Li M, Yang X, Ren J, Qu K, Qu X. Using graphene oxide high near-infrared absorbance for photothermal treatment of alzheimer's disease. *Advanced Materials*, 2012, 24(13): 1722–1728
94. Yang K, Feng L, Shi X, Liu Z. Nano-graphene in biomedicine: Theranostic applications. *Chemical Society Reviews*, 2013, 42(2): 530–547
95. Dykman L, Khlebtsov N. Gold nanoparticles in biomedical applications: Recent advances and perspectives. *Chemical Society Reviews*, 2012, 41(6): 2256–2282
96. Khlebtsov N, Dykman L. Biodistribution and toxicity of engineered gold nanoparticles: A review of *in vitro* and *in vivo* studies. *Chemical Society Reviews*, 2011, 40(3): 1647–1671
97. Ren X, Chen H, Yang V, Sun D. Iron oxide nanoparticle-based theranostics for cancer imaging and therapy. *Frontiers of Chemical Science and Engineering*, 2014, 8(3): 253–264
98. Zhang S, Sun C, Zeng J, Sun Q, Wang G, Wang Y, Wu Y, Dou S, Gao M, Li Z. Ambient aqueous synthesis of ultrasmall PEGylated Cu_{2-x}Se nanoparticles as a multifunctional theranostic agent for multimodal imaging guided photothermal therapy of cancer. *Advanced Materials*, 2016, 28(40): 8927–8936
99. Wang Y, Wu Y, Liu Y, Shen J, Lv L, Li L, Yang L, Zeng J, Wang Y, Zhang L W, et al. BSA-mediated synthesis of bismuth sulfide nanotheranostic agents for tumor multimodal imaging and thermoradiotherapy. *Advanced Functional Materials*, 2016, 26(29): 5335–5344
100. Gao F, Sun M, Xu L, Liu L, Kuang H, Xu C. Biocompatible cup-shaped nanocrystal with ultrahigh photothermal efficiency as tumor therapeutic agent. *Advanced Functional Materials*, 2017, 27(24): 1700605
101. Song S, Shen H, Yang T, Wang L, Fu H, Chen H, Zhang Z. Indocyanine green loaded magnetic carbon nanoparticles for near infrared fluorescence/magnetic resonance dual-modal imaging and photothermal therapy of tumor. *ACS Applied Materials & Interfaces*, 2017, 9(11): 9484–9495
102. Zhou B, Li Y, Niu G, Lan M, Jia Q, Liang Q. Near-infrared organic dye-based nanoagent for the photothermal therapy of cancer. *ACS Applied Materials & Interfaces*, 2016, 8(44): 29899–29905
103. Li Y, Xu N, Zhou J, Zhu W, Li L, Dong M, Yu H, Wang L, Liu W, Xie Z. Facile synthesis of a metal-organic framework nanocarrier for NIR imaging-guided photothermal therapy. *Biomaterials Science*, 2018, 6(11): 2918–2924
104. Li Y, Xu N, Zhu W, Wang L, Liu B, Zhang J, Xie Z, Liu W. Nanoscale melittin@zeolitic imidazolate frameworks for enhanced anticancer activity and mechanism analysis. *ACS Applied Materials & Interfaces*, 2018, 10(27): 22974–22984
105. Zheng C, Zheng M, Gong P, Jia D, Zhang P, Shi B, Sheng Z, Ma Y, Cai L. Indocyanine green-loaded biodegradable tumor targeting nanoprobes for *in vitro* and *in vivo* imaging. *Biomaterials*, 2012, 33(22): 5603–5609

106. Zheng M, Yue C, Ma Y, Gong P, Zhao P, Zheng C, Sheng Z, Zhang P, Wang Z, Cai L. Single-step assembly of DOX/ICG loaded lipid-polymer nanoparticles for highly effective chemophotothermal combination therapy. *ACS Nano*, 2013, 7(3): 2056–2067
107. Mordon S, Devoisselle J M, Soulie-Begu S, Desmettre T. Indocyanine green: Physicochemical factors affecting its fluorescence *in vivo*. *Microvascular Research*, 1998, 55(2): 146–152
108. Wang T, Li S, Zou Z, Hai L, Yang X, Jia X, Zhang A, He D, He X, Wang K. A zeolitic imidazolate framework-8-based indocyanine green theranostic agent for infrared fluorescence imaging and photothermal therapy. *Journal of Materials Chemistry. B, Materials for Biology and Medicine*, 2018, 6(23): 3914–3921
109. Juzeniene A, Peng Q, Moan J. Milestones in the development of photodynamic therapy and fluorescence diagnosis. *Photochemical & Photobiological Sciences*, 2007, 6(12): 1234–1245
110. Lu D, Tao R, Wang Z. Carbon-based materials for photodynamic therapy: A mini-review. *Frontiers of Chemical Science and Engineering*, 2019, 13(2): 310–323
111. Juarranz Á, Jaén P, Sanz-Rodríguez F, Cuevas J, González S. Photodynamic therapy of cancer. Basic principles and applications. *Clinical & Translational Oncology*, 2008, 10(3): 148–154
112. Henderson B W, Dougherty T J. How does photodynamic therapy work? *Photochemistry and Photobiology*, 1992, 55(1): 145–157
113. Castano A P, Demidova T N, Hamblin M R. Mechanisms in photodynamic therapy: Part one—photosensitizers, photochemistry and cellular localization. *Photodiagnosis and Photodynamic Therapy*, 2004, 1(4): 279–293
114. Xu D, You Y, Zeng F, Wang Y, Liang C, Feng H, Ma X. Disassembly of hydrophobic photosensitizer by biodegradable zeolitic imidazolate framework-8 for photodynamic cancer therapy. *ACS Applied Materials & Interfaces*, 2018, 10(18): 15517–15523
115. Xie Z, Liang S, Cai X, Ding B, Huang S, Hou Z, Ma P, Cheng Z, Lin J. O₂-Cu/ZIF-8@Ce6/ZIF-8@F127 composite as a tumor microenvironment-responsive nanoplatfrom with enhanced photo-/chemodynamic antitumor efficacy. *ACS Applied Materials & Interfaces*, 2019, 11(35): 31671–31680
116. Zhang C, Bu W, Ni D, Zhang S, Li Q, Yao Z, Zhang J, Yao H, Wang Z, Shi J. Synthesis of iron nanometallic glasses and their application in cancer therapy by a localized fenton reaction. *Angewandte Chemie International Edition*, 2016, 55(6): 2101–2106
117. Tang Z, Liu Y, He M, Bu W. Chemodynamic therapy: Tumor microenvironment-mediated fenton and fenton-like reactions. *Angewandte Chemie International Edition*, 2019, 58(4): 946–956
118. Lin L S, Song J, Song L, Ke K, Liu Y, Zhou Z, Shen Z, Li J, Yang Z, Tang W, Niu G, Yang H H, Chen X. Simultaneous Fenton-like ion delivery and glutathione depletion by MnO₂-based nanoagent to enhance chemodynamic therapy. *Angewandte Chemie International Edition*, 2018, 57(18): 4902–4906
119. Ma B, Wang S, Liu F, Zhang S, Duan J, Li Z, Kong Y, Sang Y, Liu H, Bu W, Li L. Self-assembled copper-amino acid nanoparticles for *in situ* glutathione “and” H₂O₂ sequentially triggered chemodynamic therapy. *Journal of the American Chemical Society*, 2019, 141(2): 849–857
120. Chen Y, Deng J, Liu F, Dai P, An Y, Wang Z, Zhao Y. Energy-free, singlet oxygen-based chemodynamic therapy for selective tumor treatment without dark toxicity. *Advanced Healthcare Materials*, 2019, 8(18): 1900366
121. Leader B, Baca Q J, Golan D E. Protein therapeutics: A summary and pharmacological classification. *Nature Reviews. Drug Discovery*, 2008, 7(1): 21–39
122. Chen Z, Li N, Li S, Dharmawardana M, Schlimme A, Gassensmith J J. Viral chemistry: The chemical functionalization of viral architectures to create new technology. *Wiley Interdisciplinary Reviews. Nanomedicine and Nanobiotechnology*, 2016, 8(4): 512–534
123. Mallamace F, Corsaro C, Mallamace D, Vasi S, Vasi C, Baglioni P, Buldyrev S V, Chen S H, Stanley H E. Energy landscape in protein folding and unfolding. *Proceedings of the National Academy of Sciences of the United States of America*, 2016, 113(12): 3159–3163
124. Carmichael S P, Shell M S. Entropic (de)stabilization of surface-bound peptides conjugated with polymers. *Journal of Chemical Physics*, 2015, 143(24): 243103
125. Wang C, Luan J, Tadepalli S, Liu K K, Morrissey J J, Kharasch E D, Naik R R, Singamaneni S. Silk-encapsulated plasmonic biochips with enhanced thermal stability. *ACS Applied Materials & Interfaces*, 2016, 8(40): 26493–26500
126. Liang K, Ricco R, Doherty C M, Styles M J, Bell S, Kirby N, Mudie S, Haylock D, Hill A J, Doonan C J, Falcaro P. Biomimetic mineralization of metal-organic frameworks as protective coatings for biomacromolecules. *Nature Communications*, 2015, 6(1): 7240
127. Alsaiani S K, Patil S, Alyami M, Alamoudi K O, Aleisa F A, Merzaban J S, Li M, Khashab N M. Endosomal escape and delivery of CRISPR/Cas9 genome editing machinery enabled by nanoscale zeolitic imidazolate framework. *Journal of the American Chemical Society*, 2018, 140(1): 143–146
128. Wang J, Ye Y, Yu J, Kahkoska A R, Zhang X, Wang C, Sun W, Corder R D, Chen Z, Khan S A, et al. Core-shell microneedle gel for self-regulated insulin delivery. *ACS Nano*, 2018, 12(3): 2466–2473
129. Yang J, Cao Z. Glucose-responsive insulin release: Analysis of mechanisms, formulations, and evaluation criteria. *Journal of Controlled Release*, 2017, 263: 231–239
130. Yu J, Zhang Y, Ye Y, DiSanto R, Sun W, Ranson D, Ligler F S, Buse J B, Gu Z. Microneedle-array patches loaded with hypoxia-sensitive vesicles provide fast glucose-responsive insulin delivery. *Proceedings of the National Academy of Sciences of the United States of America*, 2015, 112(27): 8260–8265
131. Chen W H, Luo G F, Vazquez-Gonzalez M, Cazelles R, Sohn Y S, Nechushtai R, Mandel Y, Willner I. Glucose-responsive metal-organic-framework nanoparticles act as “smart” sense-and-treat carriers. *ACS Nano*, 2018, 12(8): 7538–7545
132. Weed R I, Reed C F, Berg G. Is hemoglobin an essential structural component of human erythrocyte membranes? *Journal of Clinical Investigation*, 1963, 42(4): 581–588
133. Ranji-Burachaloo H, Reyhani A, Gurr P A, Dunstan D E, Qiao G

- G. Combined fenton and starvation therapies using hemoglobin and glucose oxidase. *Nanoscale*, 2019, 11(12): 5705–5716
134. Mali P, Yang L, Esvelt K M, Aach J, Guell M, DiCarlo J E, Norville J E, Church G M. Rna-guided human genome engineering via Cas9. *Science*, 2013, 339(6121): 823–826
135. Cong L, Ran F A, Cox D, Lin S, Barretto R, Habib N, Hsu P D, Wu X, Jiang W, Marraffini L A, Zhang F. Multiplex genome engineering using CRISPR/Cas systems. *Science*, 2013, 339(6121): 819–823
136. Li M, Tao Y, Shu Y, LaRochelle J R, Steinauer A, Thompson D, Schepartz A, Chen Z Y, Liu D R. Discovery and characterization of a peptide that enhances endosomal escape of delivered proteins *in vitro* and *in vivo*. *Journal of the American Chemical Society*, 2015, 137(44): 14084–14093